A Unified, Integral Construction For Coordinates Over Closed Curves

Schaefer S., Ju T. and Warren J.

Abstract

We propose a simple generalization of Shephard's interpolation to piecewise smooth, convex closed curves that yields a family of boundary interpolants with linear precision. Two instances of this family reduce to previously known interpolants: one based on a generalization of Wachspress coordinates to smooth curves and the other an integral version of mean value coordinates for smooth curves. A third instance of this family yields a previously unknown generalization of discrete harmonic coordinates to smooth curves. For closed, piecewise linear curves, we prove that our interpolant reproduces a general family of barycentric coordinates considered by Floater, Hormann and Kós that includes Wachspress coordinates, mean value coordinates and discrete harmonic coordinates.

Key words: barycentric coordinates, Shepard's interpolant, boundary value

1 Introduction

Constructing a function that interpolates known values at a set of data sites is a common problem in mathematics. Given a set of values f_j specified at a set of points p_j, the problem reduces to constructing a function $\hat{f}[v]$ such that $\hat{f}[p_j] = f_j$. Perhaps the simplest known solution to this problem is Shepard's method [1]. This interpolant has the form

$$\hat{f}[v] = \frac{\sum_j w_j f_j}{\sum_j w_j} \tag{1}$$

where the *weight* $w_j = \frac{1}{|v-p_j|}$.

The resulting function $\hat{f}[v]$ satisfies the interpolation conditions since $w_j \to \infty$ as $v \to p_j$. The final division by $\sum_j w_j$ ensures that the resulting interpolant reproduces constant functions; i.e.; if the $f_j = 1$ for all j, $\hat{f}[v] = 1$ for all v.

In computer graphics, a common variant of this interpolation problem is to specify the data f not at a finite set of sample points, but along an entire closed curve P. For example, given a set of specified colors at the vertices of a closed polygon, we extend those colors to the interior of the polygon using a function that interpolates the specified colors at the vertices and is piecewise linear along the edges of the polygon. More precisely, given a parameterization $p[x]$ for the closed curve P and a data value $f[x]$ associated with each point $p[x]$ on P, we wish to construct a function $\hat{f}[v]$ that interpolates f along P (i.e.; $\hat{f}[p[x]] = f[x]$ for all x) and behaves "reasonably" on the interior of P.

Interestingly, generalizing Shephard's method to boundary interpolation is quite straightforward. We simply replace the discrete sums of equation 1 by their corresponding integrals,

$$\hat{f}[v] = \int \frac{f[x]}{|p[x] - v|} dP / \int \frac{1}{|p[x] - v|} dP. \tag{2}$$

Again, $\hat{f}$ interpolates f on P. In particular, $\hat{f}[v] \to f[x]$ as $v \to p[x]$ since $\frac{1}{p[x]-v}$ approaches infinity. As in the discrete case, this interpolant reproduces constant functions.

Building coordinates using interpolants: Another important use of interpolants arises in applications such as mesh parameterization [2–6] and deformation [7–11] where expressing a point v as a weighted combination of the points p_j is critical. These weights are often referred to as the *coordinates* of v with respect to the p_j.

One common technique for building coordinates is to construct an interpolant that reproduces not only constant functions, but also reproduces linear functions. A discrete interpolant $\hat{f}[v]$ has *linear precision* if setting the data values f_j to be the data sites p_j yields the identity function $\hat{v} = v$. In this case, the weights w_j satisfy $v = \frac{\sum_j w_j p_j}{\sum_j w_j}$ and thus form coordinates for v with respect to the p_j. Unfortunately, Shepard's method is not suitable for constructing coordinates: the interpolant $\hat{f}[v]$ of equation 1 does not reproduce linear functions. In particular, if we set $w_j = \frac{1}{|v-p_j|}$, the weight sum $\frac{\sum_j w_j p_j}{\sum_j w_j}$ does not reproduce the point v.

Driven by the need for coordinates, there has been a large amount of research on boundary interpolants that possess *linear precision*. Such methods have the property that if $f[x] = p[x]$ for all x, $\hat{f}[v] = v$ for all v in P. The earliest work on this boundary interpolation problem is due to Wachspress [12]. The resulting *Wachspress* coordinates (defined for convex polygons) have been the subject of numerous papers that generalize these coordinates to higher dimensions and smooth convex shapes [13–15]. More recently, Floater [16] proposed an

alternative set of coordinates for any closed polygon known as *mean value* coordinates. Again, subsequent work has generalized these coordinates to higher dimensions and smooth shapes [17,11]. Finally, a third class of coordinates, *discrete harmonic* coordinates, have been used in several applications [18,19]. These coordinates arise from solving a simple variational problem involving the harmonic functional over a convex polygon P. In the case where P is a closed polygon, Floater et al. [20] have observed that all three of these coordinate constructions are instances of a more general family of 2D coordinates for closed polygons.

Interestingly, Belyaev [21] showed that barycentric coordinates are related to inverse problems in differential and convex geometry. In that paper (submitted in parallel with ours), Belyaev generates a similar extension of Wachspress and harmonic coordinates to smooth shapes and studies the ability of these coordinates to approximate harmonic functions.

Contributions: In this paper, we propose a simple modification to the continuous version of Shephard's method (given in equation 2) that yields a family of boundary interpolants with linear precision. For smooth boundary curves, the interpolant is equivalent to the integral version of Wachspress coordinates for smooth convex curves [14] when $k = 0$ and reproduces the mean value interpolant proposed in [11] when $k = 1$. For $k = 2$, the interpolant yields a previously unknown interpolant that generalizes discrete harmonic coordinates to smooth curves. For piecewise linear curves, the integral version of this interpolant reduces to a discrete sum. Based on the choice of a parameter k, this discrete method can reproduce either Wachspress coordinates ($k = 0$), mean value coordinates ($k = 1$) or discrete harmonic coordinates ($k = 2$). For arbitrary k, the integral version reduces to the family of discrete coordinates described in [20].

2 A boundary interpolant for closed curves

The following section gives a simple modification to the continuous version of Shephard's method for closed shapes (given in equation 2) that has linear precision. While the exposition in this section is entirely 2D, the integral construction extends to higher dimensions without difficulty.

2.1 The modified interpolant

Given a closed curve P with a parameterization $p[x]$ and an associated scalar function $f[x]$, we desire a function $\hat{f}[v]$ such that $\hat{f}$ interpolates f (i.e.; $\hat{f}[p[x]] =$

$f[x]$) and $\hat{f}$ reproduces linear functions. Our modification to the continuous form of Shephard's method is to perform the integrals of equation 2 with respect to a curve $\bar{P}_v$ instead of the original boundary curve P,

$$\hat{f}[v] = \int \frac{f[x]}{|p[x] - v|} d\bar{P}_v / \int \frac{1}{|p[x] - v} |d\bar{P}_v. \tag{3}$$

This *auxiliary* curve $\bar{P}_v$ depends on both the boundary curve P and the point of evaluation v. For a given v, we simply normalize each integrand by the length of the differential $d\bar{P}_v$ on $\bar{P}_v$ as the parameter x varies over P. Since $\frac{1}{|p[x]-v|}$ approaches infinity as $p[x] \to v$, the modified interpolant $\hat{f}[v]$ converges to $f[x]$ as $v \to p[x]$.

On the other hand, only certain special choices for $\bar{P}_v$ cause the modified interpolant to have linear precision. If we substitute $f[x] = p[x]$ and $\hat{f}[v] = v$ into equation 3, we observe the interpolant has linear precision if and only if the auxiliary curve $d\bar{P}_v$ satisfies

$$\int \frac{p[x] - v}{|p[x] - v|} d\bar{P}_v = 0. \tag{4}$$

In the next subsection, we construct a family of auxiliary curves $\bar{P}_v$ for which this integral is exactly zero.

2.2 A construction for the auxiliary curve

In this subsection, we give a general construction for a class of auxiliary curves $\bar{P}_v$ that satisfy equation 4. Given the closed boundary curve P and a point v, we construct the auxiliary curve $\bar{P}_v$ in two steps.

1. We translate P such that v is shifted to the origin and radially scale the shifted curve by $\frac{1}{a_v[x]}$ where $a_v[x]$ is any non-negative scalar function. This new curve P_v has a parameterization given by

$$p_v[x] = \frac{p[x] - v}{a_v[x]}.$$

2. We construct the auxiliary curve $\bar{P}_v$ by taking the *polar dual* of P_v [15]. This curve has a parameterization of the form

$$\bar{p}_v[x] = d[p_v[x]]$$

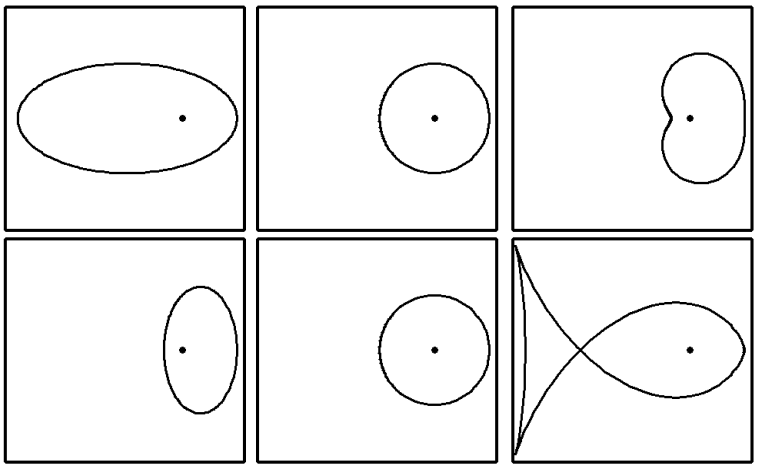

Fig. 1. Dual of an ellipse with respect to the point shown. The top row shows P_v for $k = 0, 1, 2$ (see section 3). The bottom row shows the dual of the shape above.

where the operator d computes the following:

$$d[p[x]] = \frac{p[x]^{\perp}}{p[x]^{\perp} \cdot p[x]}. \tag{5}$$

For curves, $p[x]^{\perp}$ is the outward normal vector to the curve $p[x]$ whose length is equal to that of the tangent vector $p'[x]$. (In m dimensions, we define $p[x]^{\perp}$ to the be outward normal vector formed by taking cross product of the $m-1$ tangent vectors $\frac{\partial p[x]}{\partial x_i}$.) Given that we have simply changed the integral in equation 2 to be with respect to the dual shape, we call our modified interpolant the *Dual Shepard's interpolant* or DS interpolant for short.

Figure 1 illustrates the case when the closed curve P is an ellipse with parameterization $p[x] = (2\cos[x], \sin[x])$ and the sample point v has coordinates $(1, 0)$. The three curves in the upper part of the figure are P_v where the radial scaling function $a_v[x]$ is chosen to be $|p[x] - v|^k$ with $k = 0, 1, 2$, respectively. The lower three curves are the polar duals $\bar{P}_v$ of their corresponding upper curve P_v. Observe that for $k = 2$, the radially scaled curve P_v is not convex and as a result the polar dual $\bar{P}_v$ has a self intersection. Each inflection point of P_v corresponds to a cusp on $\bar{P}_v$.

Equation 5 gives an explicit formula for computing the dual. Note that the dual curve also satisfies the following properties:

$$d[p[x]] \cdot p[x] = 1, \tag{6}$$

$$d[p[x]] \cdot \frac{\partial p[x]}{\partial x_i} = 0. \tag{7}$$

The dual $d[p[x]]$ as defined in equation 5 trivially satisfies these properties

since $p[x]^{\perp} \cdot \frac{\partial p[x]}{\partial x_i} = 0$.

The function $d[p[x]]$ is uniquely characterized by these equations as long as the the vectors $p[x]$ and $\frac{\partial p[x]}{\partial x_i}$ form a linearly independent basis, i.e; $p[x] \cdot p[x]^{\perp} \neq 0$. Geometrically, this condition corresponds to requiring that the tangent space to $p[x]$ not pass through the origin. (If the tangent space does pass through the origin at some parameter value x_0, $d[p[x]]$ goes to infinity as $x \to x_0$.)

This observation leads to the following theorem.

Theorem: Given a curve $p[x]$ whose tangent line does not pass through the origin, the dual of the dual of $p[x]$ is $p[x]$; that is, $d[d[p[x]]] = p[x]$.

Proof: We first replace $p[x]$ by $d[p[x]]$ in equations 6 and 7. If $d[d[p[x]]$ and $p[x]$ are identical, replacing $d[d[p[x]]$ by $p[x]$ in these two new equations should also yield equality; that is,

$$\begin{aligned} p[x] \cdot d[p[x]] &= 1, \\ p[x] \cdot \frac{\partial d[p[x]]}{\partial x_i} &= 0. \end{aligned}$$

The first equation follows directly from equation 6. The second equation is verified by differentiating equation 6.

$$\begin{aligned} 0 &= \frac{\partial}{\partial x_i}(d[p[x]] \cdot p[x]) \\ &= \frac{\partial d[p[x]]}{\partial x_i} \cdot p[x] + d[p[x]] \cdot \frac{\partial p[x]}{\partial x_i} \end{aligned}$$

Finally, we apply equation 7 to yield $\frac{\partial d[p[x]]}{\partial x_i} \cdot p[x] = 0$. **QED**

2.3 A proof of linear precision

We next show that the DS interpolant has linear precision. The key ingredient is to show that equation 4 reduces to an instance of the divergence theorem applied to $\bar{P}_v$. For the rest of the paper, we define $\bar{p}_v[x]$ to be the parameterization of $\bar{P}_v$ computed via $d[p_v[x]]$.

Theorem: If the radially scaled curve P_v is convex, the integral of expression 4 (with respect $d\bar{P}_v$) is identically zero.

Proof: If $\bar{p}_v[x]^\perp$ is an outward normal to $\bar{P}_v$ at $\bar{p}_v[x]$, the integral of the unitized version of this normal is exactly zero by the divergence theorem [22], i.e.;

$$\int \frac{\bar{p}_v[x]^\perp}{|\bar{p}_v[x]^\perp|} d\bar{P}_v = 0$$

Since iterating the dual operator d is the identity, the vectors $p_v[x]$ and $\bar{p}_v[x]^\perp$ are also related via the formula

$$p_v[x] = d[d[p_v[x]]] = d[\bar{p}_v[x]] = \frac{\bar{p}_v[x]^\perp}{\bar{p}_v[x]^\perp \cdot \bar{p}_v[x]}. \tag{8}$$

where $\bar{p}_v[x]^\perp \cdot \bar{p}_v[x]$ is a scalar. If P_v is convex, the polar dual $\bar{P}_v$ is also convex and this scalar expression is always non-negative. Therefore, the vectors $p[x] - v$, $p_v[x]$ and $\bar{p}_v[x]^\perp$ are all scalar multiples of each other. Thus, the unitized versions of these vectors are all equal,

$$\frac{p[x] - v}{|p[x] - v|} = \frac{p_v[x]}{|p_v[x]|} = \frac{\bar{p}_v[x]^\perp}{|\bar{p}_v[x]^\perp|}. \tag{9}$$

Direct substitution of the left-hand side of this expression into the integral yields the theorem. **QED**

When P_v is convex, $\bar{p}_v[x]^\perp \cdot \bar{p}_v[x]$ is always non-negative. However, when P_v is not convex, $\bar{p}_v[x]^\perp \cdot \bar{p}_v[x]$ may change signs. These sign changes correspond to cusps on $\bar{P}_v$ where the winding of $\bar{P}_v$ reverses with respect to the origin. (See the lower right curve in figure 1.)

In this situation, the DS interpolant of equation 3 still has linear precision as long as $d\bar{P}_v$ is treated as a signed quantity where sign of $d\bar{P}_v$ corresponds to the sign of $\bar{p}_v[x]^\perp \cdot \bar{p}_v[x]$. Since this modification entails extra complexity, we next consider an equivalent form of the DS interpolant that is easier to evaluate.

2.4 A dx form of the DS interpolant

The integrals of equations 3 and 4 were taken with respect to $d\bar{P}_v$. To facilitate evaluation of these integrals, we can rewrite the interpolant using integrals taken with respect to dx. In particular, we can replace the function $\frac{1}{|p[x]-v|}$

in equation 3 by a generic weight function $w_v[x]$ and construct an equivalent form of interpolant in terms of integrals taken with respect to dx,

$$\hat{f}[v] = \frac{\int w_v[x] f[x] dx}{\int w_v[x] dx}.$$

To construct the desired weight function, we note that from equation 8

$$\frac{p[x] - v}{a_v[x]} = \frac{\bar{p}_v[x]^\perp}{\bar{p}_v[x]^\perp \cdot \bar{p}_v[x]}.$$

Now, the differential dx and $d\bar{P}_v$ are related by the Jacobian of the parameterization $\bar{p}_v[x]$ for $\bar{P}_v$. However, by construction, the Jacobian is exactly the length of the normal vector $\bar{p}_v[x]^\perp$. Thus, $|\bar{p}_v[x]^\perp| dx = d\bar{P}_v$. Combining these two expressions yields

$$\frac{d\bar{P}_v}{|p[x] - v|} = \frac{\bar{p}_v[x]^\perp \cdot \bar{p}_v[x]}{a_v[x]} dx.$$

Substituting this expression into equation 3 yields the desired form weight function.

$$w_v[x] = \frac{\bar{p}_v[x]^\perp \cdot \bar{p}_v[x]}{a_v[x]} \tag{10}$$

Note the DS interpolant may be undefined if v lies on the tangent space of P_v for some $x = x_0$. In this case, $p_v[x_0] \cdot p_v[x_0]^\perp = 0$ and $\bar{p}_v[x_0]^\perp \cdot \bar{p}_v[x_0]$ is unbounded. Also, if $\bar{P}_v$ folds back on itself, it is possible that $\int \frac{1}{|p[x]-v|} |d\bar{P}_v = 0$ leading to an undefined interpolant. In the case of the mean value interpolant (see Sections 3 and 4), the DS interpolant is well-defined for all closed, non-intersecting shapes.

The invariance of these coordinates under different types of transformations depends on the invariance of the weight function $a_v[x]$. For example, in Sections 3 and 4, each of these coordinates are invariant under similarity transformations (translation, rotation and uniform scaling). However, when $a_v[x] = 1$, Wachspress coordinates have the added benefit of full affine invariance.

3 Equivalence to previous smooth interpolants

Our DS interpolant reproduces two known interpolants for particularly simple choices of $a_v[x]$. In particular, we consider radial scaling functions of the form

$$a_v[x] = |p[x] - v|^k.$$

For $k = 0$, our interpolant reproduces a smooth interpolant first proposed in [14] that generalizes the discrete interpolant associated with Wachspress coordinates. For $k = 1$, our interpolant reproduces the mean value interpolant first proposed in [11]. Finally, for $k = 2$, we show that our interpolant has an interpretation in terms of minimizing a certain class of ruled surfaces with respect to the harmonic functional and produces a continuous analog of discrete harmonic coordinates.

3.1 Mean value interpolation

In the process of extending mean value coordinates to 3D triangular meshes, Ju et al. [11] introduced the concept of mean value interpolation. Given a closed smooth curve P with a parameterization $p[x]$ and associated data values $f[x]$, mean value interpolation computes $\hat{f}[v]$ as the ratio of two integrals,

$$\hat{f}[v] = \int \frac{f[x]}{|p[x] - v|} dS_v / \int \frac{1}{|p[x] - v|} dS_v$$

where S_v is the unit circle centered at v.

In terms of our construction, when $k = 1$, the radially scaled curve P_v is exactly the unit circle centered at origin. Likewise, the polar dual $\bar{P}_v$ is the unit circle centered at the origin (see figure 1 middle). Since S_v and $\bar{P}_v$ are simply translates of each other, the differentials dS_v and $d\bar{P}_v$ are identical and the two interpolants agree.

3.2 Wachspress interpolation

For $k = 0$, our DS interpolant reduces to a continuous interpolant first introduced in Warren et al. [14]. This interpolant was developed in the context of extending Wachspress coordinates for convex polygons to smooth convex curves. For a closed shape P in m dimensions, Wachspress interpolation has

the form

$$\hat{f}[v] = \frac{\int w_v[x] f[x] dP}{\int w_v[x] dP} \tag{11}$$

where $w_v[x] = \frac{\kappa[x]}{(n[x]\cdot(p[x]-v))^m}$ with $\kappa[x]$ being the Gaussian curvature of P at $p[x]$ and $n[x]$ being the outward unit normal to P at $p[x]$.

As we now show, the choice of $k = 0$ (and thus $a_v[x] = 1$) for our modified Shephard's interpolant exactly reproduces Wachspress interpolation.

Theorem: Let $a_v[x] = 1$. The DS interpolant of equation 3 is equivalent to the Wachspress interpolant of equation 11.

Proof: Note that the interpolant of equation 11 can be written in dx form with a weight function

$$\frac{\kappa[x]|p_v[x]^\perp|}{(n[x]\cdot(p[x]-v))^m}.$$

Our task is show that this weight function is equivalent to the dx weight function of equation 10.

Following DoCarmo [23], Gaussian curvature at point $p[x]$ is the limit of the ratio of the area of a patch on the Gauss sphere (the sphere defined by $n[x]$) to the area of a corresponding surface patch on P as the patch size approaches zero. Mathematically, the Gaussian curvature $\kappa[x]$ satisfies

$$\kappa[x] = \frac{|n[x]^\perp|}{|p[x]^\perp|} = \frac{n[x]\cdot n[x]^\perp}{|p_v[x]^\perp|}.$$

The second equality is true because $n[x]$ is the unit normal to the sphere. Recalling that $\bar{p}_v[x]$ is exactly $\frac{n[x]}{n[x]\cdot(p[x]-v)}$ by construction, we note that

$$\bar{p}_v[x]\cdot\bar{p}_v[x]^\perp = \frac{n[x]}{n[x]\cdot(p[x]-v)}\cdot\left(\frac{n[x]}{n[x]\cdot(p[x]-v)}\right)^\perp = \frac{n[x]\cdot n[x]^\perp}{(n[x]\cdot(p[x]-v))^m}.$$

Here, the second equality holds by observing that the middle expression is a determinant with each row having a factor of $n[x]\cdot(p[x]-v)^\perp$. Extracting the m factors of this quantity from the determinant and simplifying yields the expression on the right-hand side.

To complete the proof, we combine the definition of $\kappa[x]$ with this equation and eliminate the common expression of $n[x] \cdot n[x]^{\perp}$. This combination yields

$$\frac{\kappa[x]|p_v[x]^{\perp}|}{(n[x] \cdot (p[x] - v))^m} = \bar{p}_v[x] \cdot \bar{p}_v[x]^{\perp}.$$

which is exactly the weight function associated with the dx form of our interpolant given in section 2.4. **QED**

3.3 Harmonic interpolation

For $k = 0$ and $k = 1$, our DS interpolant reproduces known smooth interpolants that themselves were developed as generalizations of known discrete interpolants for closed polygons. For $k = 2$, we know of no equivalent smooth interpolant. However, the corresponding discrete interpolant for $k = 2$ is based on *discrete harmonic* coordinates [18].

These coordinates are referred to as harmonic since the value of their associated interpolant can be defined as the result of minimizing a harmonic functional. Given a convex polygon P, linear boundary data f on the edges of P and an interior point v, consider a piecewise linear function form by radially triangulating the interior of P from v and that interpolates f on the edges of P. The value of the harmonic interpolant is now the height value of this piecewise linear surface at v that minimizes the integral of the harmonic functional of this piecewise linear function taken over P.

In this subsection, we observe that our DS interpolant has a similar interpretation in terms of harmonic minimization. Given a smooth closed $p[x]$, an associated scalar function $f[x]$ and an interior point v, consider a ruled surface formed by connecting the boundary curve $(p[x], f[x])$ to the interior point (v, f_*) where f_* is an arbitrary height at v. We can parameterize this surface via $(p[x,t], f[x,t])$ where

$$\begin{aligned} p[x,t] &= p[x](1-t) + vt, \\ f[x,t] &= f[x](1-t) + f_* t. \end{aligned}$$

Given this parameterization, we define the value of the (smooth) harmonic interpolant $\hat{f}[v]$ as

$$\hat{f}[v] = \min_{f_*} \int_P (\frac{\partial f[x,t]}{\partial v_1})^2 + (\frac{\partial f[x,t]}{\partial v_2})^2 dv_1 dv_2. \tag{12}$$

Fig. 2. Examples of interpolants created for an ellipse with a height function $v_1^2 - v_2^2$ specified on the boundary. The interpolants correspond to $k = 0$ on the top row and $k = 1, 2$ on the bottom row.

We hypothesize that our DS interpolant reproduces the harmonic interpolant of equation 12 for $k = 2$. To support this hypothesis, we make two crucial observations. First, the ruled surface $(p[x,t], f[x,t])$ in our definition of the harmonic interpolant reduces to the graph of the piecewise linear function used in the traditional construction of discrete harmonic coordinates when P is a closed polygon. Second, as, we shall show in the next section, our DS interpolant (with $k = 2$) reproduces discrete harmonic coordinates for closed polygons. Furthermore, we have numerically verified that our coordinates satisfy equation 12 for our elliptical test case in figure 2.

Figure 2 shows three examples of the DS interpolant applied to our ellipse from figure 1. The upper left figure shows a 3D view of the space curve $(p[x], f[x])$ where the scalar function $f[x]$ is $4\cos[x]^2 - \sin[x]^2$. The remaining three figures shows a graph generated by applying DS interpolation to interior of the ellipse. In the case of Wachspress interpolation and harmonic interpolation, the interpolant was computed by evaluating the integral of equation 2 in closed form using Mathematica for a undetermined point v and evaluating the resulting expression for grid of values of v.

4 Equivalence to previous discrete interpolants

In this section we investigate the behavior of the DS interpolant when the curve P as well as the associated function f are piecewise linear. Let P be a $2D$ polygon with vertices $\{p_0, p_1, \ldots, p_n = p_0\}$ and function values $\{f_0, f_1, \ldots, f_n = f_0\}$. Furthermore, associated with each point parameter values $\{x_0, x_1, \ldots, x_n = x_0\}$ such that

$$\begin{aligned} p[x] &= \tfrac{(x_i - x)p_{i-1} + (x - x_{i-1})p_i}{x_i - x_{i-1}} \qquad \text{for } x_{i-1} \le x \le x_i \\ f[x] &= \tfrac{(x_i - x)f_{i-1} + (x - x_{i-1})f_i}{x_i - x_{i-1}} \qquad \text{for } x_{i-1} \le x \le x_i. \end{aligned} \tag{13}$$

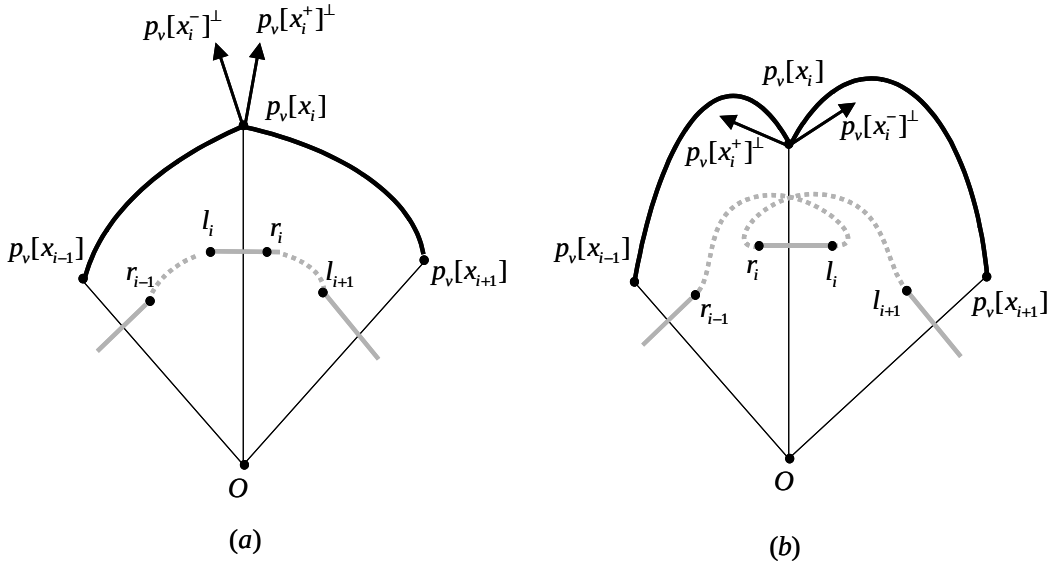

Fig. 3. Convex (a) and concave (b) vertices of P_v (dark) and their corresponding pieces on $\bar{P}_v$ (gray and dashed). The vertices l_i and r_i of $\bar{P}_v$ correspond to the two distinct normals to P_v at $p_v[x_i]$.

Our goal is to reduce our interpolant to the discrete form $\hat{f}[v] = \frac{\sum_i w_i f_i}{\sum_i w_i}$ where the weights w_i depend on v. In particular, we show that our integral construction reproduces a family of barycentric coordinates first described in Floater et al. [20].

4.1 Structure of the dual

We first consider the structure of the dual $\bar{P}_v$ for piecewise linear shapes. To construct the polar dual of a shape with normal discontinuities, we treat a point on the curve that exhibits this discontinuity as an infinite collection of points at the same location but with smoothly varying normals. Let $p_v[x_i^-]^\perp$ and $p_v[x_i^+]^\perp$ be the normal vectors of $p_v[x_i]$ on its left and right curve segments (see figure 3). Interestingly, by representing $p_v[x_i]$ as an infinite collection of points with normals varying continuously from $p_v[x_i^-]^\perp$ to $p_v[x_i^+]^\perp$, the polar dual of $p_v[x_i]$ forms a straight line segment with end points at

$$l_i = \frac{p_v[x_i^-]^\perp}{p_v[x_i^-]^\perp \cdot p_v[x_i]}$$
$$r_i = \frac{p_v[x_i^+]^\perp}{p_v[x_i^+]^\perp \cdot p_v[x_i]}$$

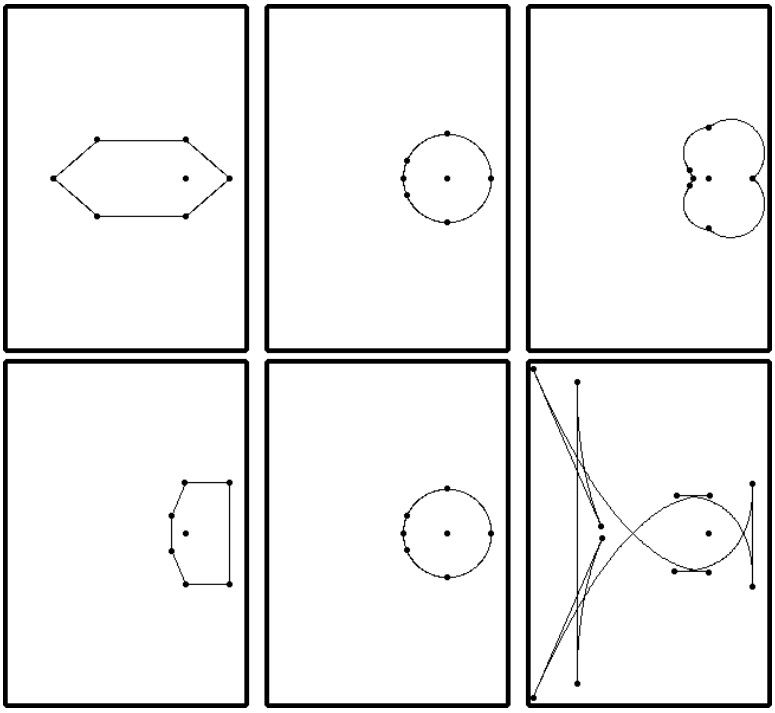

Fig. 4. Examples of duals of a ellptical hexagon with respect to the point shown. The top row shows P_v for $k = 0, 1, 2$. The bottom row shows the dual of the shape above.

When $p_v[x_i]$ forms a concave corner, the location of l_i and r_i with respect to p_i may be reversed as shown in figure 3 (b). Figure 4 shows a discrete version of the ellipse from figure 1 sampled at intervals of $\frac{\pi}{3}$. The top row illustrates P_v for different values of k while the bottom row shows the corresponding dual $\bar{P}_v$. When $k \neq 0$, P_v is curved as is the dual $\bar{P}_v$. Notice that when P_v is not convex, $\bar{P}_v$ may fold back and self-intersect as shown in the bottom-right corner.

Now we can describe the structure of the polar dual $\bar{P}_v$ in relation to the polygon P. As shown in figure 3 (a), $\bar{P}_v$ is composed of two types of segments: curved segments between $\{r_{i-1}, l_i\}$ corresponding to each edge $\{p_{i-1}, p_i\}$ and straight segments $\{l_i, r_i\}$ corresponding to each vertex p_i. In order to parameterize $\bar{P}_v$, we let l_i and r_i correspond to parameters x_i^- and x_i^+, that is, $l_i = \bar{p}_v[x_i^-]$ and $r_i = \bar{p}_v[x_i^+]$. Using this structure of the dual and equation 13, we can rewrite the numerator of equation 3 in the form

$$\sum_i \int_{x_{i-1}^+}^{x_i^-} \frac{f_{i-1}(1-t) + f_i t}{|p[x] - v|} d\bar{P}_v + \sum_i \int_{x_i^-}^{x_i^+} \frac{f_i}{|p[x] - v|} d\bar{P}_v \tag{14}$$

where $t = \frac{x - x_{i-1}^+}{x_i^- - x_{i-1}^+}$.

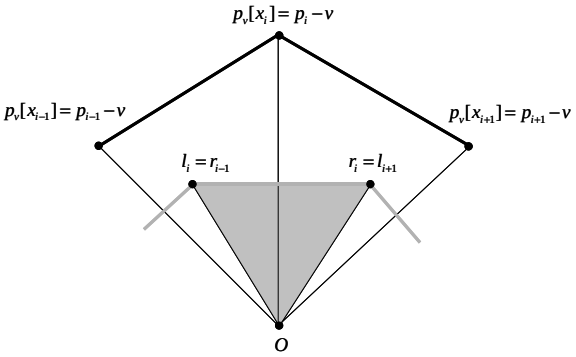

Fig. 5. The dual for Wachspress coordinates is a piecewise linear shape where $l_i = r_i$. The discrete weight for these coordinates is proportional to the area of the shaded wedge on the dual.

We then use this piecewise definition of the interpolant $\hat{f}[v]$ to rewrite the integral equation as a discrete sum $\hat{f}[v] = \frac{\sum_i w_i f_i}{\sum_i w_i}$ where $w_i = \alpha_i + \beta_i + \gamma_i$ and

$$\alpha_i = \int_{x_i^+}^{x_{i+1}^-} \frac{1-t}{|p[x]-v|} d\bar{P}_v \qquad \beta_i = \int_{x_{i-1}^+}^{x_i^-} \frac{t}{|p[x]-v|} d\bar{P}_v \qquad \gamma_i = \int_{x_i^-}^{x_i^+} \frac{1}{|p[x]-v|} d\bar{P}_v.$$

4.2 Equivalence to Wachspress

To give more intuition about the shape of the auxiliary curve $\bar{P}_v$, we first look at the special case when $a_v[x]$ is the identity function and $p_v[x] = p[x] - v$. Notice that the normal vectors $p_v[x_i^-]^\perp$ and $p_v[x_i^+]^\perp$ now become the outward unit normals of the edges $\{p_{i-1}, p_i\}$ and $\{p_i, p_{i+1}\}$. Furthermore, by applying the definition of the dual from equation 5 to this piecewise linear shape, we find that $r_{i-1} = l_i$. As a result, the polar dual $\bar{P}_v$ consists solely of straight segments $\{l_i, r_i\}$ as shown in figures 4(left) and 5.

Since $x_i^+ = x_{i+1}^-$, $\alpha_i = \beta_i = 0$. γ_i is also easy to calculate because $\frac{1}{|p[x]-v|} = \frac{1}{|p_i-v|}$ over $\{x_i^-, x_i^+\}$. Therefore, $\gamma = \frac{|l_i - r_i|}{|p_i - v|}$, which is proportional to the area of the shaded wedge in figure 5. This relation to the area of the dual is exactly the same as the discrete definition of Wachspress coordinates given by Ju et al. [15].

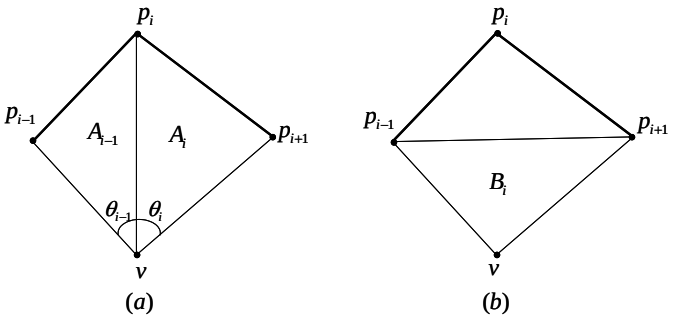

Fig. 6. The areas of triangles formed by the vertices of P and v for Floater's family of barycentric coordinates.

4.3 Equivalence to Floater's family of coordinates

Floater et al. [20] considers a general family of barycentric coordinates for $2D$ polygons with weights w_i of the form

$$w_i = \frac{c_{i-1}}{A_{i-1}} + \frac{c_{i+1}}{A_i} - \frac{c_i B_i}{A_{i-1} A_i}$$

where A_i is the signed area of the triangle $\{v, p_i, p_{i+1}\}$, B_i is the signed area of the triangle $\{v, p_{i-1}, p_{i+1}\}$ and c_i is an arbitrary scalar associated with the vertex p_i as shown in figure 6. Furthermore, the authors show that given any set of weights w_i' that are barycentric coordinates, there exists choices of c_i such that $w_i = w_i'$. In other words, this family of coordinates can reproduce all possible discrete barycentric coordinates. In particular, if $c_i = |p_i - v|^k$, these coordinates reproduce Wachspress coordinates when $k = 0$, mean value coordinates when $k = 1$ and discrete harmonic coordinates when $k = 2$.

Theorem: The DS interpolant of equation 3 reproduces Floater's family of coordinates if $a_v[x_i] = c_i$.

Proof: We begin by using the properties of the dual to relate vertices of $\bar{P}_v$ to the vertices P using $\alpha_i, \beta_i, \gamma_i$. To do so, we overload the $\perp$ operator to apply to vectors as well as functions. If z is a vector in $2D$ from the origin, we define $z^\perp$ to be the vector z rotated counter-clockwise by $\frac{\pi}{2}$ radians.

Consider the quantity $\alpha_i(p_i - v) + \beta_{i+1}(p_{i+1} - v)$. Based on the definition of α_i and β_{i+1} in terms of integrals (as well as equation 13), this quantity is exactly

$$\alpha_i(p_i - v) + \beta_{i+1}(p_{i+1} - v) = \int_{x_i^+}^{x_{i+1}^-} \frac{p[x] - v}{|p[x] - v|} d\bar{P}_v.$$

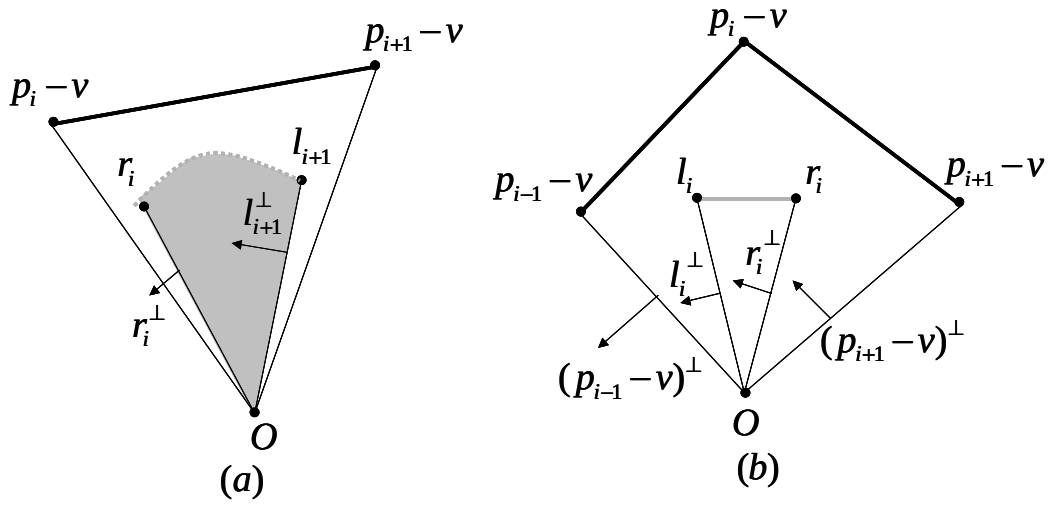

Fig. 7. The dual $\bar{P}_v$ in relation to P. $l_i^{\perp}$ and $r_i^{\perp}$ are the corresponding vectors rotated counter-clockwise by $\frac{\pi}{2}$ radians.

Now, as shown in section 2.3, the right-hand side of this expression is exactly the integral of the outward unit normal of $\bar{P}_v$ restricted to the interval $[x_i^+, x_{i+1}^-]$ (i.e; the dotted curve from r_i to l_{i+1} in figure 7(a)). If we apply the divergence theorem to the shaded wedge in figure 7(a), this integral itself is exactly equal to difference of the vectors $l_{i+1}^{\perp}$ and $r_i^{\perp}$. So, in summary, we have derived an equation relating the vector $p_i - v$ to the vectors l_i and r_i.

$$\alpha_i(p_i - v) + \beta_{i+1}(p_{i+1} - v) = l_{i+1}^{\perp} - r_i^{\perp}. \tag{15}$$

Using a similar argument, we can show that

$$\gamma_i(p_i - v) = r_i^{\perp} - l_i^{\perp}.$$

We can solve for α_i in closed form by dotting both sides of equation 15 with $(p_{i+1} - v)^{\perp}$ and dividing the result by $(p_i - v) \cdot (p_{i+1} - v)^{\perp} = 2A_i$,

$$\alpha_i = \frac{l_{i+1}^{\perp} \cdot (p_{i+1} - v)^{\perp} - r_i^{\perp} \cdot (p_{i+1} - v)^{\perp}}{(p_i - v) \cdot (p_{i+1} - v)^{\perp}} = \frac{a_v[x_{i+1}] - r_i^{\perp} \cdot (p_{i+1} - v)^{\perp}}{2A_i},$$

where A_i is defined as in figure 6. The second equality is due to the identity $l_{i+1}^{\perp} \cdot (p_{i+1} - v)^{\perp} = l_{i+1} \cdot (p_{i+1} - v) = \bar{p}_v[x_{i+1}^+] \cdot (p_v[x_{i+1}]a_v[x_{i+1}]) = a_v[x_{i+1}]$. Similarly, we can solve for β_i and γ_i.

$$\beta_i = \frac{a_v[x_{i-1}] - l_i \cdot (p_{i-1} - v)^{\perp}}{2A_{i-1}}$$
$$\gamma_i = \frac{(r_i^{\perp} - l_i^{\perp}) \cdot (p_i - v)}{|p_i - v|^2}$$

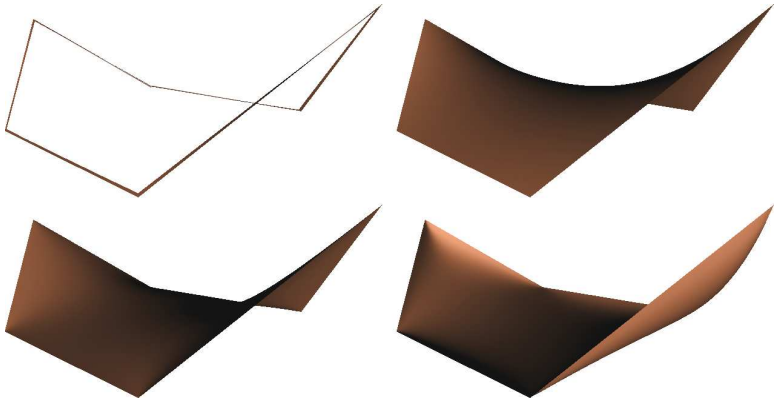

Fig. 8. Examples of interpolants created for a discrete piecewise linear elliptical hexagon with height values specified at the vertices. The interpolants correspond to $k = 0$ on the top row and $k = 1, 2$ on the bottom row.

To find the weight $w_i = \alpha_i + \beta_i + \gamma_i$ we use the above equalities and apply trigonometric identities to obtain

$$\begin{aligned}\alpha_i + \beta_i + \gamma_i &= \frac{a_v[x_{i-1}]}{2A_{i-1}} + \frac{a_v[x_{i+1}]}{2A_i} - \frac{a_v[x_i](\cos[\theta_{i-1}]\sin[\theta_i] + \cos[\theta_i]\sin[\theta_{i-1}])}{|p_i - v|^2 \sin[\theta_i]\sin[\theta_{i-1}]} \\ &= \frac{a_v[x_{i-1}]}{2A_{i-1}} + \frac{a_v[x_{i+1}]}{2A_i} - \frac{a_v[x_i]B_i}{2A_{i-1}A_i}\end{aligned}$$

Since we chose $a_v[x_i] = c_i$, this completes the proof of equivalence to Floater's family of coordinates. **QED**

Figure 8 shows three examples of DS interpolant applied to the elliptical hexagon of figure 2.

5 Conclusion and future work

The main usefulness of the Dual Shephard interpolant proposed here is that it gives a simple conceptual framework for understanding a range of interpolants developed for generating 2D coordinates. This interpolant readily generalizes to higher dimensions and, in future work, we intend to investigate the usefulness of this interpolant in constructing coordinates for closed 3D shapes. For example, we may be able to develop coordinates for closed, piecewise polynomial curves and surfaces. In this case, we believe that computing closed form solutions to the integral of equation 3 should be possible. Such an extension would allow curved shapes to be used as control meshes for defining deformations (as done in [11] for triangular meshes).

References

[1] D. Shepard, A two-dimensional interpolation function for irregularly-spaced data, in: Proceedings of the 1968 23rd ACM national conference, ACM Press, 1968, pp. 517–524.

[2] K. Hormann, G. Greiner, MIPS - An Efficient Global Parametrization Method, in: Curves and Surfaces Proceedings (Saint Malo, France), 2000, pp. 152–163.

[3] M. Desbrun, M. Meyer, P. Alliez, Intrinsic Parameterizations of Surface Meshes, Computer Graphics Forum 21 (3) (2002) 209–218.

[4] A. Khodakovsky, N. Litke, P. Schröder, Globally smooth parameterizations with low distortion, ACM Trans. Graph. 22 (3) (2003) 350–357.

[5] J. Schreiner, A. Asirvatham, E. Praun, H. Hoppe, Inter-surface mapping, ACM Trans. Graph. 23 (3) (2004) 870–877.

[6] M. S. Floater, K. Hormann, Surface parameterization: a tutorial and survey, in: N. A. Dodgson, M. S. Floater, M. A. Sabin (Eds.), Advances in Multiresolution for Geometric Modelling, Mathematics and Visualization, Springer, Berlin, Heidelberg, 2005, pp. 157–186.

[7] T. W. Sederberg, S. R. Parry, Free-form deformation of solid geometric models, in: SIGGRAPH '86: Proceedings of the 13th annual conference on Computer graphics and interactive techniques, ACM Press, 1986, pp. 151–160.

[8] S. Coquillart, Extended free-form deformation: a sculpturing tool for 3d geometric modeling, in: SIGGRAPH '90: Proceedings of the 17th annual conference on Computer graphics and interactive techniques, ACM Press, 1990, pp. 187–196.

[9] R. MacCracken, K. I. Joy, Free-form deformations with lattices of arbitrary topology, in: SIGGRAPH '96: Proceedings of the 23rd annual conference on Computer graphics and interactive techniques, ACM Press, 1996, pp. 181–188.

[10] K. G. Kobayashi, K. Ootsubo, t-ffd: free-form deformation by using triangular mesh, in: SM '03: Proceedings of the eighth ACM symposium on Solid modeling and applications, ACM Press, 2003, pp. 226–234.

[11] T. Ju, S. Schaefer, J. Warren, Mean Value Coordinates for Closed Triangular Meshes, in: ACM Trans. on Graphics (SIGGRAPH Proceedings), 2005, pp. 561–566.

[12] E. Wachspress, A Rational Finite Element Basis, Manuscript.

[13] J. Warren, Barycentric Coordinates for Convex Polytopes, Advances in Computational Mathematics 6 (1996) 97–108.

[14] J. Warren, S. Schaefer, A. Hirani, M. Desbrun, Barycentric coordinates for convex sets, To appear in Advances in Computational and Applied Mathematics.

[15] T. Ju, S. Schaefer, J. Warren, M. Desbrun, A Geometric Construction of Coordinates for Convex Polyhedra using Polar Duals, in: ACM/EG Symposium on Geometry Processing, 2005, pp. 181–186.

[16] M. Floater, Mean value coordinates, Computer Aided Geometric Design 20 (2003) 19–27.

[17] M. S. Floater, G. Kós, M. Reimers, Mean value coordinates in 3d, Computer Aided Geometric Design 22 (2005) 623–631.

[18] U. Pinkall, K. Polthier, Computing discrete minimal surfaces and their conjugates, Experimental Mathematics 2 (1) (1993) 15–36.

[19] M. Eck, T. DeRose, T. Duchamp, H. Hoppe, M. Lounsbery, W. Stuetzle, Multiresolution analysis of arbitrary meshes, in: Proceedings of SIGGRAPH '95, 1995, pp. 173–182.

[20] M. Floater, K. Hormann, G. Kós, A general construction of barycentric coordinates over convex polygons, To appear in Advances in Computational Mathematics.

[21] A. Belyaev, On transfinite barycentric coordinates, in: ACM/EG Symposium on Geometry Processing, 2006, pp. 89–99.

[22] W. Fleming, Functions of Several Variables, Springer-Verlag, 1977.

[23] M. DoCarmo, Differential geometry of curves and surfaces, Prentice-Hall, 1976.